Applications in Engineering Science 7 (2021) 100053

Contents lists available at ScienceDirect

Applications in Engineering Science

journal homepage: www.elsevier.com/locate/apples

A peculiar value of M to M_{cr} ratio: Reconsidering assumptions of curvature analysis of reinforced concrete beams

Gintaris Kaklauskas [a,*], Aleksandr Sokolov [b]

[a] Department of Reinforced Concrete Structures and Geotechnique, Vilnius Gediminas Technical University (VilniusTech), Vilnius, Lithuania
[b] Laboratory of Innovative Building Structures, Vilnius Gediminas Technical University (VilniusTech), Vilnius, Lithuania

ARTICLE INFO

Keywords:
RC beam
Curvature
Effective moment of inertia
Deflection
Cracked section
Statistics

ABSTRACT

The paper critically evaluates design code techniques (ACI 318-14, ACI 318-19, and Eurocode 2) for the instantaneous curvature analysis of reinforced concrete (RC) beams. The study examines the soundness of the assumption that a fully cracked section represents the lower bound of the effective moment of inertia (or bending stiffness) used along with the hypothesis of plane sections. Experimental RC beams were investigated to find a load corresponding to the stiffness of a fully cracked section. The load was identified as a condition when the resultant tension stiffening force, inversely calculated from the test moment-curvature response, equals zero. The conducted analysis showed that for the majority of the experimental beams, the stiffness of a fully cracked section was reached at a bending moment of $3M_{cr}$ (with M_{cr} defined by ACI 318), irrespective of the geometrical and material characteristics of the beams. As these results conflict with the abovementioned hypothesis regarding the lower bound of bending stiffness, the hypothesis was reformulated accordingly, and a new curvature model was proposed. A comparison of the predicted and experimental curvatures of 69 RC beams reported in the literature demonstrates the superiority of the proposed model over the design code techniques.

1. Introduction

At the early stage of development of the theory of reinforced concrete (RC), deformation problems were simply ignored. The first attempts of predicting deflection were based on the principles of the theory of elasticity. Deflection was accurately predicted only at the load stage preceding cracking. After cracking, deflection was grossly underestimated, particularly that of lightly reinforced members. From an analogy with the ultimate limit state, it was rightly assumed that in the cracked section the tensile stresses were resisted by the reinforcement alone, and thus, it was further presupposed that tensile concrete makes no contribution to the stiffness of RC members. However, deflection analysis based on the geometrical characteristics of a fully cracked section that excludes the area of concrete in tension gave no more accurate results. In this case, predictions overestimated the real values which was again particularly evident for lightly reinforced members.

Early experimental studies scientifically investigating the contribution of reinforcement and concrete to the stiffness of cracked RC members were conducted at the end of the nineteenth century. Considere (1899) reported the results of load – deformation behaviour of small mortar prisms reinforced with steel wires. The performed tests have shown that deformation response was stiffer compared to that of the bare steel bar. In the discussion of the latter tests, Morsch (1909) suggested that concrete between cracks is capable of carrying tensile stresses, thus reducing strain in the reinforcement and contributing to the overall stiffness of the member. This phenomenon was later called tension stiffening by implying the enhanced stiffness in regard to the fully cracked state (Gilbert and Warner, 1978; Belarbi and Hsu, 1994). Tension stiffening is induced by bond stresses acting at the concrete-reinforcement interface. Between the adjacent cracks of a reinforced concrete element, tensile stress is transferred from the reinforcement to concrete by bond. Tension stiffening to a significant extent affects stiffness, crack spacing and crack width characteristics.

The further development of deflection prediction methods, that included the effect of tension stiffening, was quite independently carried out in the East (Murashev, 1950) and in the West (Branson, 1965). In Russia, Murashev (1950) has developed an ingenious curvature model of the flexural cracked RC members. It was based on the hypothesis of plane sections and accounted for nonlinear strains of the compressive concrete and the non-uniform distribution of reinforcement strains due to cracking. The latter effect, in the Western countries known as tension stiffening, was assessed by factor ψ_s, expressing the ratio of mean reinforcement strain to reinforcement strain in the cracked section.

Branson (1965) proposed a rational and simple deflection calculation approach for RC bending members, which is the best-known model in the West. He suggested a concept of the effective moment of inertia,

* Corresponding author.
E-mail address: Gintaris.Kaklauskas@vilniustech.lt (G. Kaklauskas).

https://doi.org/10.1016/j.apples.2021.100053
Received 4 February 2021; Received in revised form 14 April 2021; Accepted 15 April 2021
Available online 21 April 2021

I_e, adopted by the ACI 318 Building Code in 1971. The model was in use until 2019 when an alternative formula for I_e was recommended (ACI 318-19, 2019). Branson's approach was also adopted in the codes of Canada, Australia, New Zealand, and a number of countries in South America. Interestingly, even a European country (Spain) introduced the Branson's model to the national design standards during the period from 1991 to 2008. The model rests on these four assumptions:

1) Under flexural deformation, the member cross-section remains planar and has a linear strain distribution across its depth.
2) The moment of inertia of uncracked section, I_g, represents the upper bound of the effective moment of inertia, I_e.
3) The moment of inertia of a fully cracked section, I_{cr}, is considered the lower bound of the effective moment of inertia, I_e.
4) Elastic properties are assumed for both concrete and reinforcement.

The effective moment of inertia represents a gradual transition from I_g to I_{cr} (ACI 318-14, 2014):

$$I_e = \left(\frac{M_{cr}}{M}\right)^3 I_g + \left[1 - \left(\frac{M_{cr}}{M}\right)^3\right] I_{cr} \tag{1}$$

M is the bending moment under consideration. The gross moment of inertia of uncracked section, I_g, is calculated ignoring reinforcement. The cracking moment is calculated as for the elastic section (ACI 318-14, 2014; ACI 318-19, 2019):

$$M_{cr} = \frac{f_r I_g}{y_t} \tag{2}$$

where y_t is the distance from the tension face to the centroid of the section (for rectangular section, $y_t = 0.5h$); f_r is the rupture modulus of concrete calculated as (ACI 318-19, 2019):

$$f_r = 0.623\lambda\left(f_c\right)^{0.5} \text{ [MPa]} \tag{3}$$

where f_c is the cylinder strength. For normal-weight concrete, $\lambda = 1$.

In ACI 318-19 (2019), the elasticity modulus of concrete is expressed as

$$E_c = 4700\left(f_c\right)^{0.5} \text{ [MPa]} \tag{4}$$

Curvature is in inverse relation to the moment of inertia, I, and bending stiffness, EI. Due to cracking, the moment of inertia, I, varies along the RC member. To calibrate the effective moment of inertia, I_e (see Eq. (1)), Branson (1965) assumed a constant value of the modulus of elasticity (E_c) with curvature being expressed as $\kappa = M/E_c I_e$.

Accurate deflection prediction is performed through double integration of curvature considering shear deformations. However, in everyday design, simple calculation formulas are preferred. For instance, for a simply supported beam, deflection is expressed through the curvature calculated at a maximum bending moment, span, and a factor taking into account loading conditions. In the simplified calculations of deformations of RC beams, due to a close relationship of the effective moment of inertia, I_e, flexural stiffness, $E_c I_e$, curvature, κ, and deflection, f, these terms are frequently used in a similar context.

It is important to note that Eq. (1) was empirically derived from the test data on the simply supported RC beams having a reinforcement ratio between 1% and 2%. A number of studies (e.g., Gilbert, 1999; Scanlon et al., 2001; Gribniak et al., 2013) have shown that Bransons' model significantly underestimated curvatures/deflections of the experimental members having low reinforcement ratios ($\rho < 0.5\%$).

Aiming to remedy deflection predictions of lightly reinforced members, Bischoff (2005) proposed an alternative relationship of the effective moment of inertia based on the fundamental concepts of tension stiffening postulated in (CEB, 2013):

$$I_e = \frac{I_{cr}}{1 - \left(\frac{M_{cr}}{M}\right)^2\left[1 - \frac{I_{cr}}{I_g}\right]} \le I_g \tag{5}$$

Bischoff and Scanlon (2007) have shown that tension stiffening incorporated in Eq. (5) is independent of the reinforcement ratio (or I_{cr}/I_g ratio). Gilbert (2006) has demonstrated that the predictions of lightly reinforced members using Eq. (5) were significantly improved compared to ACI 318-14 (2014). The above model was adopted by ACI 318-19. Scanlon and Bischoff (2008) suggested using a reduced cracking moment equal to the two-thirds of M_{cr} value specified in ACI 318-14 to account for the tensile restraint stress in concrete due to shrinkage. When $M \le \frac{2}{3}M_{cr}$, $I_e = I_g$ and when $M > \frac{2}{3}M_{cr}$, the effective moment of inertia, I_e, is expressed as (ACI 318-19, 2019)

$$I_e = \frac{I_{cr}}{1 - \left(\frac{\left(\frac{2}{3}\right)M_{cr}}{M}\right)^2\left[1 - \frac{I_{cr}}{I_g}\right]} \le I_g \tag{6}$$

Eurocode 2 (CEN, 2004) and CEB (2013) suggest a model similar to the one proposed by Branson (1965). A reinforced concrete member is divided into two regions: uncracked (*region I*) and fully cracked (*region II*). The average curvature is expressed via the interpolation between the uncracked and fully cracked regions:

$$\kappa = (1 - \zeta)\kappa_1 + \zeta\kappa_2 \tag{7}$$

where κ_1 and κ_2 are the curvatures in *regions I*, and *II*, respectively. Coefficient ζ indicates how close the stress and strain state is to the condition causing cracking. It takes a value of zero at the cracking moment and approaches unity at the advanced loading stages:

$$\zeta = 1 - \beta\left(\frac{M_{cr}}{M}\right)^2 \tag{8}$$

where β is a factor taken as 1.0 for the case of short-term loading.

The prediction accuracy of short-term curvatures of RC beams and slabs of the design code techniques was discussed in Gribniak et al. (2013). It was shown that accuracy in terms of the mean values and the coefficient of variation varied significantly (in a statistical sense) with a change in reinforcement ratio and load intensity. More accurate results were achieved in the case when moderate and high reinforcement ratios were considered. High scatter was characteristic of low reinforcement ratios ($\rho < 0.4\%$) and early cracking stages.

This paper critically evaluates design code techniques (ACI 318 and Eurocode 2) for the instantaneous curvature analysis of RC beams. The study examines the soundness of the assumption that the fully cracked section represents the lower bound of bending stiffness used along with the hypothesis of plane sections. For experimental RC beams, it is demonstrated that the bending stiffness of a fully cracked section is reached at a bending moment of approximately $3M_{cr}$, irrespective of the geometrical and material characteristics. As these results are in conflict with the assumption that a fully cracked section represents the lower limit of flexural stiffness, the presumption is revised accordingly. Based on the revised assumption, new models for curvature and the effective moment of inertia are proposed. Then, the model is validated against test data and design code techniques.

2. Calculation of the resultant tension-stiffening force

This section examines the soundness of Assumption 3 (see Introduction) used along with the hypothesis of plane sections (Assumption 1). For that purpose, an investigation on experimental RC beams was performed to identify a load corresponding to the stiffness of a fully cracked section. The resultant tension stiffening force, N_{ts}, was inversely calculated from the equilibrium equations based on the test moment-curvature response. The load at which tension stiffening force equals zero ($N_{ts} = 0$) represents the fully cracked state.

The calculation of N_{ts} is illustrated in Fig. 1. The resultant tension stiffening force is obtained by an inverse technique based on the curvature response of experimental RC beams, as suggested by Kaklauskas et al. (2011b) and Salys (2011). Following the reinforcement-related tension stiffening approach proposed by Gilbert and Warner (1978), the inverse technique assumes that the resultant tension stiffening force acts at the centroid of tensile reinforcement (Fig. 1c).

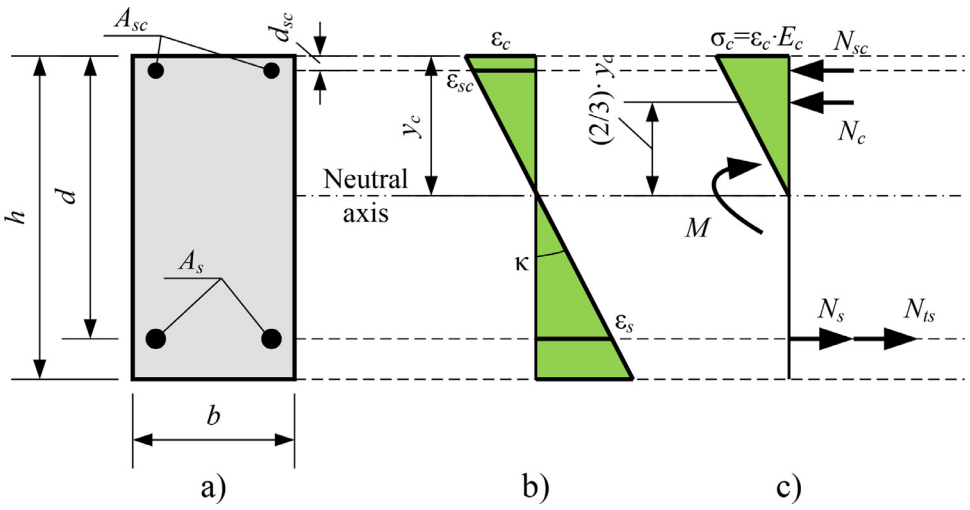

Fig. 1. Doubly reinforced section subjected to external bending: (a) cross-section; (b) strain compatibility; (c) stresses, internal forces, and external bending moment.

Torres et al. (2015) proposed a closed-form solution for calculating reinforcement-related tension stiffening stresses for bending RC members. Following (Kaklauskas and Ghaboussi, 2001; Kaklauskas and Gribniak, 2011), Kaklauskas and Gribniak (2016) suggested a procedure for considering the shrinkage effect on the moment-curvature diagram and the resultant tension stiffening force of the experimental RC beams.

To make the results of the conducted analysis compatible with Branson's approach, the inverse technique employs the hypothesis of plane sections and assumes elastic properties for reinforcement and compressive concrete. The stresses acting in the tensile concrete (elastic ones and stresses due to tension stiffening and tension softening) are modelled by the resultant internal force herein termed as the *resultant tension stiffening force*, N_{ts} (Fig. 1c).

The expressions of the inverse technique given below follow the formulae from Torres et al. (2015) and Kaklauskas and Gribniak (2016). Equilibrium equations of internal forces and bending moments with respect to tension reinforcement are as follows:

$$N_s + N_{ts} - N_c - N_{sc} = 0 \tag{9}$$

$$N_c\left(d - \frac{y_c}{3}\right) + N_{sc}\left(d - d_{sc}\right) - M = 0 \tag{10}$$

where N_s, and N_{sc} are the internal forces of tension and compressive reinforcement; N_c is the internal force of compressive concrete; M is the external bending moment. Other characteristics are evident from Fig. 1.

Equilibrium Eqs. (9) and (10) can be expressed in terms of characteristic strains (ε_c, ε_s and ε_{sc}) related to the respective internal forces as shown in Fig. 1:

$$N_{ts} + \varepsilon_s E_s A_s - \varepsilon_c \frac{E_c y_c b}{2} - \varepsilon_{sc} E_{sc} A_{sc} = 0 \tag{11}$$

$$\varepsilon_c \frac{E_c y_c b}{2}\left(d - \frac{y_c}{3}\right) + \varepsilon_{sc} E_{sc}\left(d - d_{sc}\right) A_{sc} - M = 0 \tag{12}$$

where ε_c, ε_s, and ε_{sc} are the strains of the compressive concrete (extreme fibre) and tensile and compressive reinforcement, respectively. Based on the assumption of plane sections, the latter strains can be related to curvature:

$$\kappa = \frac{\varepsilon_c}{y_c} = \frac{\varepsilon_{sc}}{y_c - d_{sc}} = \frac{\varepsilon_s}{d - y_c} \tag{13}$$

Along with the characteristic strains expressed through curvature, the moment equilibrium Eq. (12) can be transformed into the form:

$$\kappa \frac{E_c y_c^2 b}{2}\left(d - \frac{y_c}{3}\right) + \kappa E_{sc}\left(d - d_{sc}\right)\left(y_c - d_{sc}\right) A_{sc} - M = 0 \tag{14}$$

The above expression can serve as the key equation for inverse analysis. For M and κ values taken from the test, Eq. (14) produces a single unknown, namely, neutral axis depth, y_c. Eq. (14) can be rearranged in the cubic form (Kaklauskas and Gribniak, 2016) as

$$C_0 + C_1 y_c + C_2 y_c^2 + C_3 y_c^3 = 0 \tag{15}$$

$$C_0 = -\kappa E_{sc} A_{sc} d_{sc}\left(d - d_{sc}\right) - M \tag{16}$$

$$C_1 = \kappa E_{sc} A_{sc}\left(d - d_{sc}\right) \tag{17}$$

$$C_2 = \frac{\kappa E_c b d}{2} \tag{18}$$

$$C_3 = -\frac{\kappa E_c b}{6} \tag{19}$$

The cubic equation has three roots. Discarding negative and imaginary roots, the one satisfying condition $0 < y_c \le h$ can be obtained from the equations below:

$$y_c = -\frac{\left[2\left(C_2^2 - 2C_3 C_1\right)0.5\sin\Theta + C_2\right]}{3C_3} \tag{20}$$

$$\Theta = \frac{1}{3}\sin^{-1}\left[\frac{9C_3 C_2 C_1 - 27C_3^2 C_0 - 2C_2^3}{2\left(C_2^2 - 2C_3 C_1\right)^{1.5}}\right] \tag{21}$$

The resultant tension stiffening force can be then expressed from Eqs. (11) to (13):

$$N_{ts} = \kappa\left[\frac{E_c y_c^2 b}{2} + E_{sc}\left(y_c - d_{sc}\right) A_{sc} - E_s\left(d - y_c\right) A_s\right] \tag{22}$$

The calculation of tension stiffening force versus the bending moment applying the above technique is illustrated in Fig. 2. The experimental moment-curvature diagrams of six RC beams of a rectangular section taken from different experimental programs are shown in Fig. 2a. The beams were subjected to four-point loading. The main geometrical and material characteristics are given in Table 1 and include section height, reinforcement ratio, and compressive strength ranging within the extended intervals. Section height varied from 0.2 to 0.5 m, reinforcement ratio – from 0.3% to 1.9%, and compressive strength – from 18 MPa to 50 MPa. The calculated normalized tension stiffening diagrams for beams S3-2-3, S2-3, and S1-2, having nominally the same material and geometrical characteristics, except for the reinforcement ratio (and bar diameter, see Table 1), are given in Fig. 2b. The bending moment was normalized with respect to the cracking moment, whereas tension stiffening force was expressed in terms of $N_{ts}/(f_r bh)$. The results of the remaining beams, along with the specimens of the first group, are

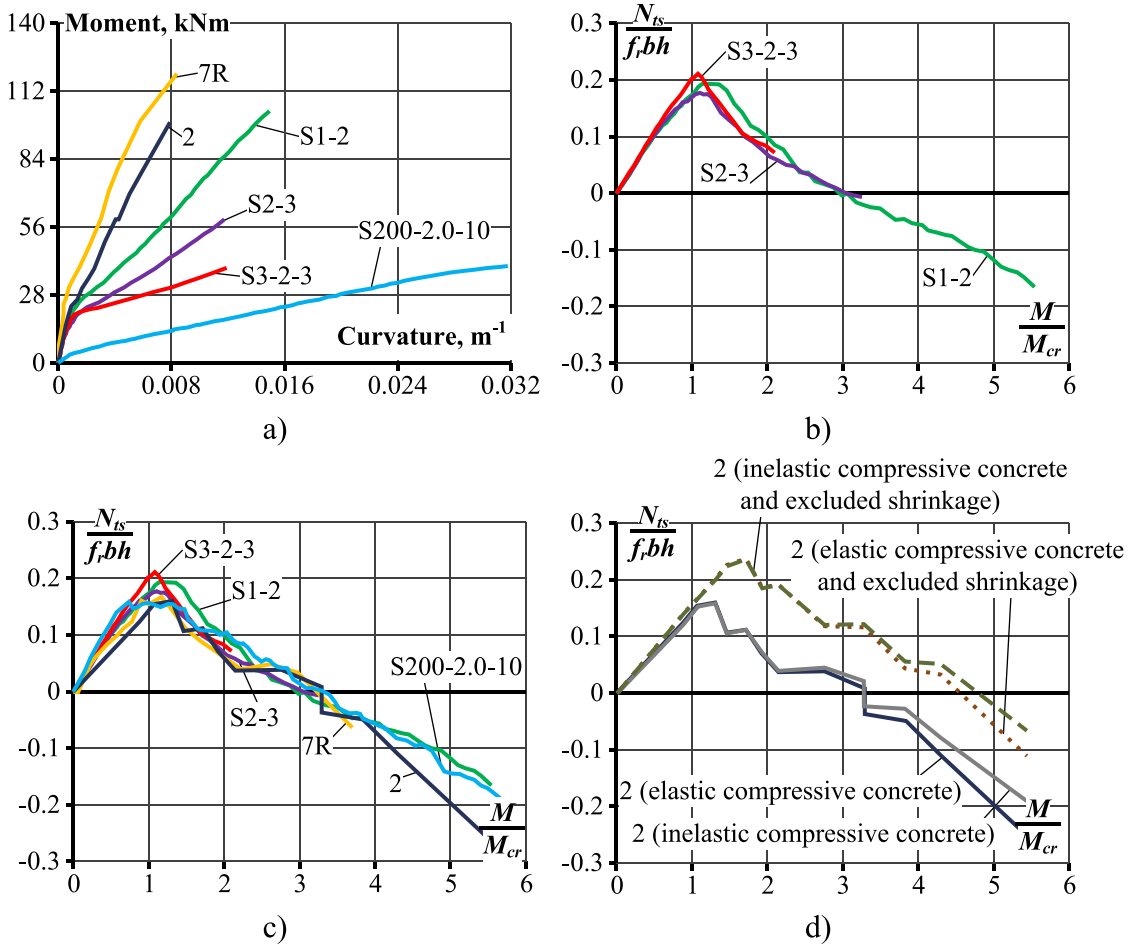

Fig. 2. Deriving tension stiffening relations from test moment-curvature diagrams: (a) moment-curvature diagrams; (b) normalized tension stiffening force for beams with ranging reinforcement ratio; (c) normalized tension stiffening force for beams with ranging reinforcement ratio, section height and concrete grade; (d) the effect of shrinkage and nonlinear strains of compressive concrete.

Table 1
Main characteristics of RC specimens analysed.

Specimen	h	b	d	d_{sc}	A_s	A_{sc}	ρ	f_y	E_s	E_{sc}	f_c
		mm			mm^2		%	MPa	GPa		MPa
S3-2-3	298	284	271	32	232	57	0.3	578	210	200	50.9
S2-3	300	282	272	29	466	57	0.6	632	211	200	48.1
S1-2	300	284	273	29	777	57	1.0	632	211	200	49.4
2	408	203	363	35	942	101	1.3	274	206	206	26.6
7R	511	204	473	32	603	101	0.6	300	206	206	23.4
S200-2.0-10	198	212	149	28	619	56	2.0	500	203	202	50.9

given in Fig. 2c. Needed for the analysis f_r and E_c, were calculated by the ACI code using Eqs. (3) and (4). The following conclusions are made with reference to the results presented in Fig. 2b and c:

1) Very similar tension stiffening force – moment relations were obtained for beams S3-2-3, S2-3, and S1-2 (see Fig. 2b) having roughly the same material and geometrical characteristics, except for the reinforcement ratio (Table 1). The most important finding was that, irrespective of the reinforcement ratio, the condition of $N_{ts}=0$ for each of the beams was reached at a load level of approximately $M/M_{cr}=3$. Note that extrapolation was needed to define the latter value for beam S3-2-3, which had the lowest reinforcement ratio ($\rho=0.3\%$).
2) Due to difference in the reinforcement ratio, tension stiffening force – moment relations attained different maximum M/M_{cr} values (see Fig. 2b). The higher was the reinforcement ratio, the higher M/M_{cr} value was reached.
3) The results of the second group of the beams having different section heights, reinforcement ratios, and compressive strength values exhibited similar tendencies: tension stiffening force – moment relations crossed the horizontal axis at coordinates close to $M/M_{cr}=3$.
4) For the cases when reinforcement ratio was above 0.6%, the $N_{ts}-M$ relations had portions of negative values. This opposes the concept of tension stiffening being associated with tensile stresses. The higher was the reinforcement ratio, the more significant was the portion of the negative tension stiffening force.

The reasons for producing negative N_{ts} values by the inverse technique can be as follows:

Table 2
Main characteristics of the beams.

Test programs	Number of beams	h, mm	b, mm	d, mm	d/h	ρ, %	f_c, MPa
Clark and Speirs (1978)	14	202–513	202–204	167–480	0.82–0.94	0.45–1.98	18.4–31.7
Figarovskij (1962)	8	248–252	179–180	223–232	0.90–0.92	0.25–0.88	17.7–30.4
Artemjev (1959)	10	252–263	176–187	222–235	0.88–0.90	0.80–0.91	21.3–47.9
Gribniak (2009)	4	299–301	277–283	274–281	0.92–0.93	0.38–0.40	37.8–44.4
Kaklauskas et al. (2008)	16	298–305	275–285	248–279	0.83–0.92	0.30–1.02	44.2–52.8
Kaklauskas et al. (2011a)	10	152–304	275–283	116–278	0.74–0.92	0.58–1.47	31.4–44.6
Kaklauskas et al. (2019)	7	198–606	212–312	149–565	0.75–0.93	0.32–1.96	50.4–52.5
Total:	69	198–606	176–312	116–565	0.74–0.94	0.25–1.98	17.7–52.8

a) The hypothesis of plane sections might not be strictly accurate for calculating the mean curvatures of bending RC members. With the imposed hypothesis of plane sections, the inverse technique overestimated the internal force of tensile reinforcement, N_s. To compensate for the latter inaccuracy and maintain the equilibrium of internal forces and bending moments, tension stiffening force, N_{ts}, had to be reduced at the expense of the overestimation of N_s. This could be the reason why N_{ts} enters an interval of negative values for the members having a higher reinforcement ratio.
b) Inelastic strains in the compressive concrete had an effect on curvatures and N_{ts}. The effect was most pronounced for the cases of a high reinforcement ratio, a low concrete grade, and advanced loading stages. Fig. 2d shows an example of the $N_{ts} - M$ relation (see the grey solid line) calculated for beam 2 (Table 2), assuming the parabolic stress-strain relationship of Eurocode 2 for compressive concrete. Fig. 2d demonstrates that the inclusion of nonlinear strains had a relatively negligible effect on N_{ts} with a slight reduction in the negative part of the relation.
c) Concrete shrinkage had an effect on the moment-curvature diagram and tension stiffening force, N_{ts}. Due to the restraining action of reinforcement, shrinkage induced tensile stresses in concrete, resulting in lower crack resistance and larger deformations of RC members (Ghali et al., 1986). Kaklauskas and Gribniak (2011, 2016) proposed a technique for eliminating shrinkage effect from both moment-curvature and tension stiffening relations of bending RC members. Fig. 2d shows a tension stiffening relation (see dotted line) for beam 2 with excluded shrinkage effect. The dashed line represents tension stiffening behaviour when both shrinkage effect and the inelastic strains of compressive concrete were taken into account. With shrinkage being dominant, the two effects notably reduced negative stresses; however, considerable portions of negative values remained.

The results given in Fig. 2(b and c) are clearly in conflict with Assumption 3 (see Introduction), which states that a fully cracked section represents the lower limit of flexural stiffness. It was demonstrated that for members with an average or high reinforcement ratio, the bending stiffness of a fully cracked section was reached at a bending moment that could be more than twice smaller than the service value. Based on the above findings, a simple model of curvature and the effective moment of inertia will be proposed in the next section.

3. New models for curvature and the effective moment of inertia

The above analysis of experimental RC beams based on the hypothesis of plane sections showed that Assumption 3 (see Introduction) was not satisfied. The bending stiffness of a fully cracked section for the experimental RC beams was reached at a bending moment close to $3M_{cr}$ (with M_{cr} calculated by the ACI code), irrespective of the reinforcement ratio, section height, and concrete grade. Bending stiffness further decreased with an increase in the load that may be up to 2 to 3 times greater than $3M_{cr}$ for the RC sections having moderate and high reinforcement ratios. However, even though Assumption 3 has not been satisfied, there is no basis for concluding it is incorrect. The authors

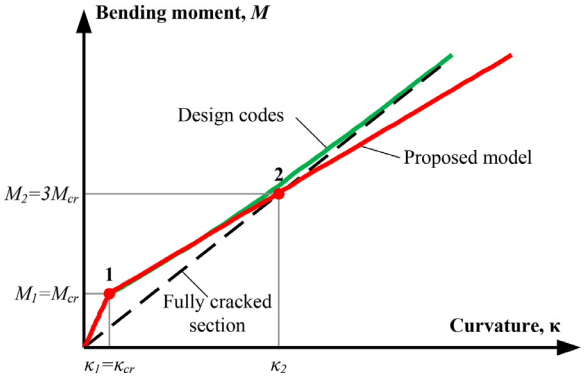

Fig. 3. The proposed curvature model.

do think that Assumption 3 on its own is a sound and rational presumption relating the effective moment of inertia (or bending stiffness) to the simple concept of a fully cracked section. On the other hand, despite the considerations that the hypothesis on plane sections might be responsible for introducing an error in the mean curvature analysis, abandoning this hypothesis does not seem rational, as it makes the analysis simple and versatile. Thus, it was decided to retain the hypothesis on plane sections but to modify Assumption 3 revised in the following way:

Assumption 3. The moment of inertia of the RC bending section reaches the value of I_{cr} at a bending moment of $3M_{cr}$.

For the approaches that do not specifically deal with the effective moment of inertia, the above assumption may take a more general form:

The fully cracked response (curvature, stiffness) is reached at a bending moment of $3M_{cr}$.

Further new formulae for calculating mean curvature and the effective moment of inertia are given. The approach is illustrated in Fig. 3, showing a moment-curvature diagram with points 1 and 2 representing cracking moment $M_1 = M_{cr}$ and bending moment $M_2 = 3M_{cr}$, respectively. Following the revised Assumption 3, it is presumed that the bending stiffness of the fully cracked section (E_cI_{cr}) is reached at bending moment M_2. Based on linear interpolation between moments M_1 and M_2, curvature can be then calculated from the below expression:

$$\kappa = \kappa_1 + \frac{(\kappa_2 - \kappa_1)(M - M_1)}{(M_2 - M_1)} \tag{23}$$

where M is the bending moment under consideration; κ_1 and κ_2 are the curvatures calculated at bending moments M_1 and M_2, respectively.

Assuming that $M_2 = 3M_{cr}$ and simplifying, Eq. (23) gets the shape:

$$\kappa = \kappa_1 + 0.5(\kappa_2 - \kappa_1)(M/M_1 - 1) \tag{24}$$

Similarly, the effective moment of inertia can be expressed as:

$$I_e = I_1 + 0.5(I_2 - I_1)(M/M_1 - 1) \tag{25}$$

Following notations from ACI 318, Eq. (25) takes the form:

$$I_e = I_g + 0.5(I_{cr} - I_g)(M/M_{cr} - 1) \tag{26}$$

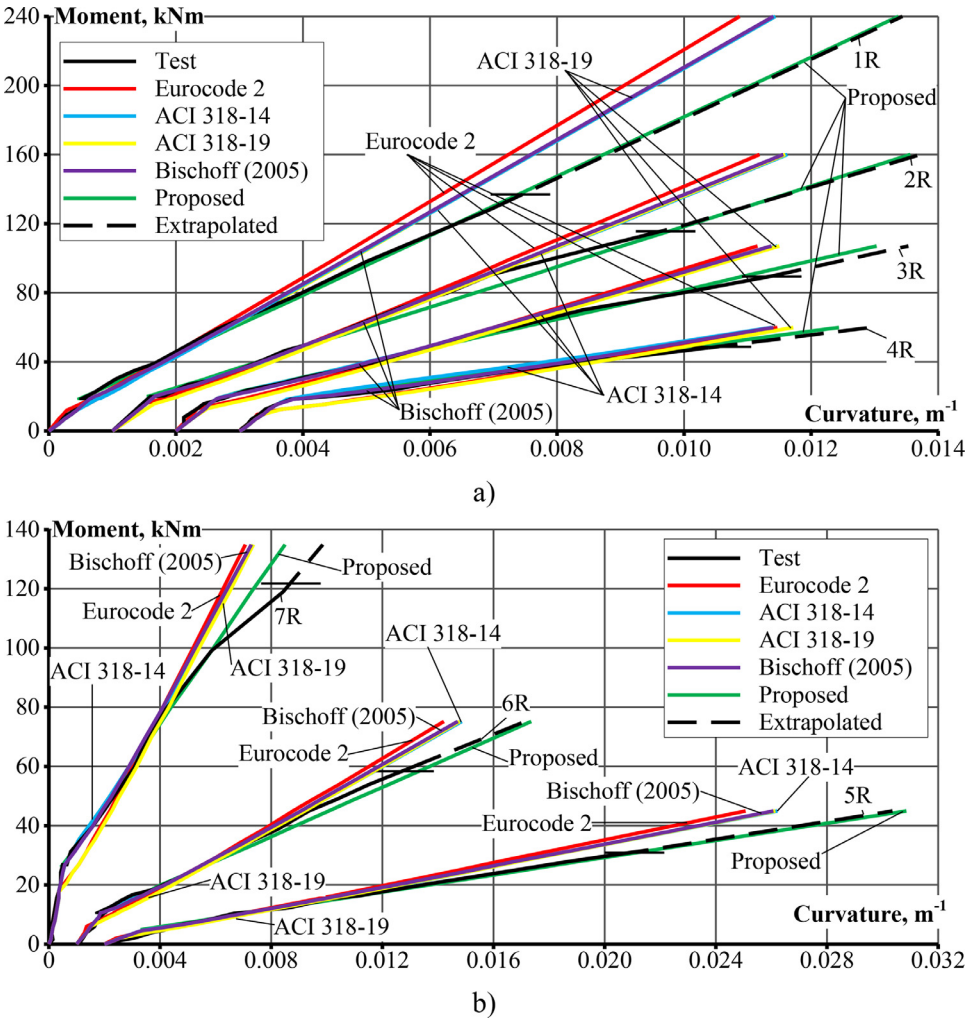

Fig. 4. The predicted curvatures for the test RC beams reported by Clark and Speirs (1978): (a) beams 1R, 2R, 3R and 4R; (b) beams 5R, 6R and 7R.

Table 3
Main nominal characteristics of selected test beams.

Specimen	h, mm	b, mm	d, mm	Ø, mm	A_s, mm^2	ρ, %	f_y, MPa	E_s, GPa	f_c, MPa
1R	412	202	368	25	1473	1.98	318	206	27.8
2R	408	204	367	20	942	1.26	274	206	31.7
3R	409	204	376	16	603	0.79	300	206	29.2
4R	406	204	370	12	339	0.45	300	206	24.9
5R	202	202	169	16	603	1.77	300	206	28.2
6R	308	203	273	16	603	1.09	300	206	27.3
7R	511	204	473	16	603	0.63	300	206	23.4
P1-2Pk	248	180	223	7	102	0.25	620	200	17.7
S3-2-3	298	284	271	10	232	0.30	578	210	50.9

where $I_1 = I_g$ is the moment of inertia of uncracked gross section (reinforcement is ignored); $I_2 = I_{cr}$ is the moment of inertia of a fully cracked section.

The numerical results of curvature analysis depend on the assumed properties of concrete such as elasticity modulus, E_c, and tensile strength (or rupture modulus, f_r). As characteristic point $M_2 = 3M_{cr}$ was established using ACI-318 formulas for f_r and E_c [see Eqs. (3) and (4), respectively], the same expressions are employed in curvature analysis.

Eqs. (23)–(26) include parameters M_1, κ_1, and κ_2. Cracking moment M_1 is calculated using this ACI-318 formula:

$$M_1 = M_{cr} = \frac{f_r I_1}{y_t} \tag{27}$$

where y_t is the distance from the centroid of the gross section to the extreme tension fibre.

Curvatures κ_1 and κ_2 are defined from the below simple equations:

$$\kappa_1 = \frac{M_1}{E_c I_1} = \frac{M_{cr}}{E_c I_g} \tag{28}$$

$$\kappa_2 = \frac{M_2}{E_c I_2} = \frac{3M_{cr}}{E_c I_{cr}} \tag{29}$$

4. Comparison of curvature predictions to tests and design code techniques

This section compares instantaneous curvature predictions of the proposed model against test data on RC beams reported in the literature. The comparison also includes curvature models from ACI 318-14, ACI 318-19, Eurocode 2 and Bischoff (2005).

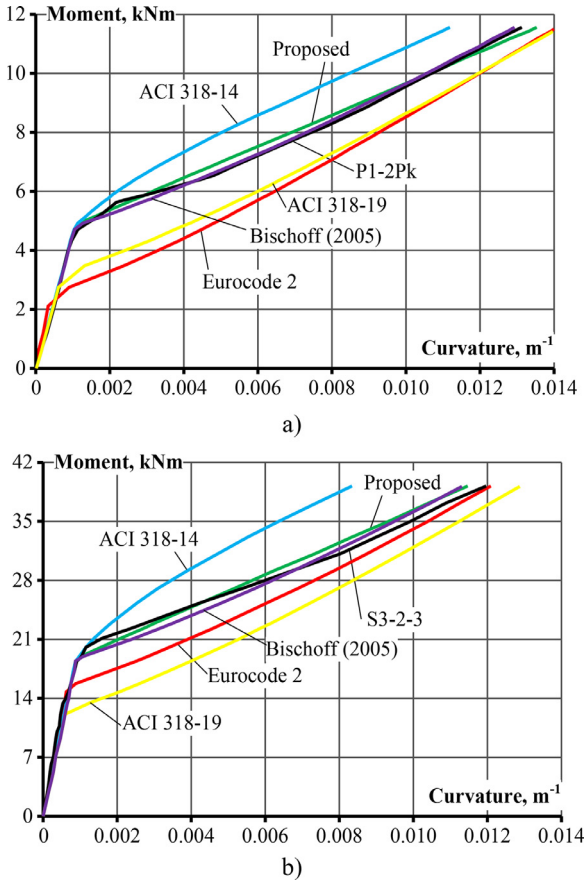

Fig. 5. Characteristic predicted moment-curvature diagrams for lightly reinforced beams (a) P1-2Pk (Figarovski, 1962); (b) S3-2-3 (Kaklauskas et al., 2008).

The study employed seven experimental programs of RC beams of rectangular section (69 specimens) subjected to four-point bending. All the beams were reinforced with ribbed bars. The majority of the experiments (Clark and Speirs, 1978; Kaklauskas et al., 2008; Gribniak, 2009; Kaklauskas et al., 2011a, 2019) can be categorized as highly accurate tests on curvatures measured via mean strain recordings on the surface of the beams at several (3 to 4) section height levels along the pure bending zone. Curvatures for the remaining beams (Figarovskij, 1962; Artemjev, 1959) were obtained from the deflection of the central point. Variations in the main geometrical and material characteristics of the beams such as section height h, width, b, effective depth, d, the d/h ratio, reinforcement ratio, ρ, and cylinder strength, f_c, are given in Table 2. For most of the specimens, the d/h ratio was close to 0.9, which is a typical value of RC beams.

An illustration of curvature predictions of the proposed model and code techniques is presented in Figs. 4 and 5. Fig. 4 shows prediction results of the tests conducted by Clark and Speirs (1978). While the latter study reports curvature results of seven couples of twin specimens (14 RC beams altogether), Fig. 4 presents the results of seven duplicate specimens noted by "R". The main nominal geometrical and material characteristics of the beams are given in Table 3. The specimens largely represent the cases of a medium and high reinforcement ratio; beam 4R only had a reinforcement ratio below 0.5%. The specimens were split into two series. In the first one (beams 1R to 4R), section height was held constant, but bar diameter and thus the reinforcement ratio varied, whereas, in the second series, the steel area was kept constant, but the overall depth changed. The moment-curvature diagrams of the first and second series are depicted in Fig. 4a and b, respectively. Curvature predictions of the proposed model for all beams were more accurate than the remaining techniques. The difference was particularly evident for the members having a higher reinforcement ratio. There was a general tendency that curvatures predicted by design codes and Bischoff's model underestimated the test values at load levels above $3M_{cr}$. The greater is the M/M_{cr} ratio, the larger is the deviation.

Fig. 5 shows the characteristic predicted moment-curvature diagrams of beams P1-2Pk and S3-2-3 having small reinforcement ratios (0.25 and 0.3%, respectively). The main geometrical and material characteristics of these beams are given in Table 3. In general, the ACI 318-14 technique underestimated the curvatures of lightly reinforced members, whereas the ACI 318-19 and Eurocode 2 models grossly overestimated curvatures at the early post-crack stages. The predictions of the proposed and Bischoff's models were very close to each other and to the test results.

A comparison of the predicted versus test curvatures was performed based on the procedure suggested by Gribniak et al. (2013). Predictions were expressed in terms of the normalized curvatures:

$$\bar{\kappa} = \frac{\kappa_{th}}{\kappa_{exp}} \tag{30}$$

where κ_{th} and κ_{exp} are the predicted and experimental curvatures, respectively.

As curvature predictions of RC bending members to a significant extent are affected by the loading level and reinforcement ratio (Gribniak et al., 2013), calculations were performed at different load levels and reinforcement ratio intervals. The load level was expressed in terms of the normalized bending moment linearly ranging between cracking and yield points:

$$\bar{M} = \frac{M - M_y}{M_y - M_1} \tag{31}$$

where M_y is the yield bending moment assuming that yield stress of tensile reinforcement $f_y = 500$ MPa.

The current study considered six load levels:

$$\bar{M} = \{0; 0.2; 0.4; 0.6; 0.8; 1\}$$

where $\bar{M} = 0$ and $\bar{M} = 1$ represent cracking (M_{cr} assessed by Eqs. (2) and (3)) and yielding points, respectively. It should be pointed out that some of beam tests were terminated before the members reached M_y. For these specimens, missing $\bar{M}$ points were obtained by means of extrapolation. Test data were grouped into three reinforcement ratio intervals:

1) $\rho < 0.5\%$ (22 *beams*); 2) $0.5 \le \rho \le 1.2\%$ (35 *beams*);
3) $\rho > 1.2\%$ (12 *beams*)

Under the assumption of the above intervals, basic statistics were calculated at each normalized load level. Table 4 presents mean normalized curvature, $\bar{\kappa}$, and the coefficient of variation, CV. A graphical illustration of the analysed results in terms of 95% of the confidence intervals of the normalized curvature is given in Fig. 6 where the scatter of predictions was characterized by the width of confidence intervals. The following conclusions can be drawn with reference to the results presented in Table 4 and Fig. 6:

1) The mean values and the coefficient of variation differed in the considered curvature models and also changed for different reinforcement ratios and load intensities. Greater scatter was obtained by all the methods when cases of low reinforcement ratio and early cracking stages were considered.
2) In support of the results of the previous studies (Gilbert, 2001; Bischoff, 2005; Gribniak et al., 2013), the ACI 318-14 model significantly underestimated the curvatures of lightly reinforced members ($\rho < 0.5\%$). The new ACI code (ACI 318-19, 2019) is free of the above shortcoming: it considerably overestimated the curvatures, particularly at the early stage of cracking. In fact, for various reinforcement ratios and load intensities, ACI 318-19 demonstrated very similar tendencies in curvature predictions to those of Eurocode 2.

Table 4
Basic statistics (mean and coefficient of variation) for curvature predictions grouped by reinforced ratio and load intervals.

$\overline{M}$	Eurocode 2	ACI 318-14	ACI 318-19	Bischoff	Proposed
	Mean (CV)	Mean (CV)	Mean (CV)	Mean (CV)	Mean (CV)
			$\rho <$ **0.5%**		
0	2.628 (0.255)	0.942 (0.227)	3.386 (0.804)	0.942 (0.227)	0.942 (0.227)
0.2	2.041 (0.370)	0.866 (0.288)	2.461 (0.805)	1.341 (0.308)	1.187 (0.300)
0.4	1.446 (0.353)	0.738 (0.251)	1.656 (0.711)	1.128 (0.273)	1.033 (0.248)
0.6	1.182 (0.229)	0.704 (0.236)	1.306 (0.550)	1.006 (0.174)	0.959 (0.156)
0.8	1.078 (0.174)	0.713 (0.222)	1.169 (0.452)	0.962 (0.132)	0.948 (0.122)
1	0.995 (0.132)	0.719 (0.242)	1.063 (0.363)	0.917 (0.119)	0.931 (0.133)
Total	**1.562 (0.485)**	**0.778 (0.268)**	**1.840 (0.593)**	**1.056 (0.268)**	**1.000 (0.234)**
			0.5 $\leq \rho \leq$ **1.2%**		
0	1.587 (0.241)	0.910 (0.245)	1.924 (0.596)	0.910 (0.245)	0.910 (0.245)
0.2	1.131 (0.182)	0.939 (0.204)	1.219 (0.312)	1.032 (0.172)	0.993 (0.170)
0.4	0.984 (0.120)	0.920 (0.153)	1.035 (0.170)	0.957 (0.116)	0.997 (0.117)
0.6	0.928 (0.105)	0.908 (0.123)	0.968 (0.124)	0.924 (0.098)	1.011 (0.096)
0.8	0.891 (0.107)	0.890 (0.111)	0.924 (0.113)	0.897 (0.097)	1.014 (0.089)
1	0.862 (0.112)	0.870 (0.110)	0.891 (0.112)	0.872 (0.102)	1.010 (0.092)
Total	**1.064 (0.298)**	**0.906 (0.167)**	**1.160 (0.374)**	**0.932 (0.164)**	**0.990 (0.143)**
			$\rho >$ **1.2%**		
0	1.129 (0.253)	0.854 (0.215)	1.381 (0.469)	0.854 (0.215)	0.854 (0.215)
0.2	0.971 (0.096)	0.975 (0.094)	1.028 (0.110)	0.970 (0.087)	0.993 (0.087)
0.4	0.904 (0.072)	0.935 (0.065)	0.945 (0.067)	0.924 (0.062)	1.019 (0.061)
0.6	0.862 (0.077)	0.895 (0.067)	0.897 (0.068)	0.886 (0.065)	1.016 (0.065)
0.8	0.839 (0.078)	0.871 (0.067)	0.871 (0.068)	0.865 (0.066)	1.015 (0.068)
1	0.803 (0.071)	0.834 (0.066)	0.834 (0.066)	0.830 (0.066)	0.989 (0.064)
Total	**0.918 (0.183)**	**0.893 (0.118)**	**0.993 (0.236)**	**0.888 (0.116)**	**0.977 (0.116)**
All beams	**1.197 (0.460)**	**0.863 (0.203)**	**1.348 (0.575)**	**0.965 (0.214)**	**0.990 (0.176)**

3) At higher loads, the design codes and Bischoff's model underestimated the curvatures of the beams having moderate and high reinforcement ratios. As the current study included only a limited number of specimens having a high reinforcement ratio, future studies should aim to investigate heavily reinforced members.
4) The proposed model demonstrated consistent prediction results, with the mean normalized curvature being approximately unity, independent of the load level (except for cracking point, $\bar{M} = 0$) and reinforcement ratio. In most cases, the proposed model also showed superiority over design code techniques in terms of the coefficient of variation. Future studies should be dedicated to improving the predictions of crack resistance.
5) The predictions of Bischoff's technique for lightly reinforced members ($\rho < 0.5\%$) were similar to the ones of the proposed model, whereas for the beams having a moderate and large reinforcement ratio, they were almost identical with the results obtained in line to ACI 318-14.

5. Future studies

The current study considered short-term curvature tests on the beams having rectangular sections reinforced with steel bars. For most of the specimens, the d/h ratio was close to 0.9, which is a typical value of RC beams. Future studies should consider the cases of fibre-reinforced polymer (FRP) and hybrid reinforcement, long-term loading, nonrectangular sections, and a d/h ratio of 0.8, which is characteristic of slabs. Improvements in calculating M_{cr} should be made.

6. Conclusions

The paper critically evaluated design code techniques for the instantaneous curvature analysis of RC beams and suggested new models for curvature and the effective moment of inertia. Based on the findings of the study, the following conclusions can be made:

1) With a gradual reduction in tension stiffening and bending stiffness after crack initiation, the stiffness of a fully cracked section of the experimental RC beams was reached at a bending moment close to $3M_{cr}$ (with M_{cr} calculated by the ACI code), irrespective of the reinforcement ratio, section height, and concrete grade. Bending stiffness further decreased with increasing load, that may be several times greater than $3M_{cr}$ for RC sections with moderate and high reinforcement ratios. This finding is clearly in conflict with the assumption that a fully cracked section represents the lower limit of flexural stiffness.
2) The resultant tension stiffening force calculated by an inverse technique from the test moment-curvature response of an RC member under the imposed hypothesis of plane sections, may reach negative values at loads above $3M_{cr}$. At the advanced load levels, negative tension stiffening force may well exceed the maximum positive value. As tension stiffening is naturally associated with tensile stress, negative stress implies that the hypothesis of plane sections might not be strictly accurate for mean curvature analysis.
3) Despite considerations that the hypothesis of plane sections might be responsible for introducing an error in the analysis of mean curvature, abandoning this hypothesis does not seem rational, as it makes the analysis versatile and straightforward. Therefore, it was decided to retain the hypothesis of plane sections. However, the assumption stating that a fully cracked section represents the lower bound of bending stiffness was revised suggesting that the stiffness of a fully cracked section is reached at a bending moment of $3M_{cr}$.
4) Following the above assumption, a simple formula was proposed for calculating instantaneous curvature and the effective moment of inertia based on linear interpolation between the curvature points at M_{cr} and $3M_{cr}$.

The study explored the predictive capabilities of the proposed model by comparing the calculated instantaneous curvatures against test data on RC beams. The data set represented seven experimental programs of

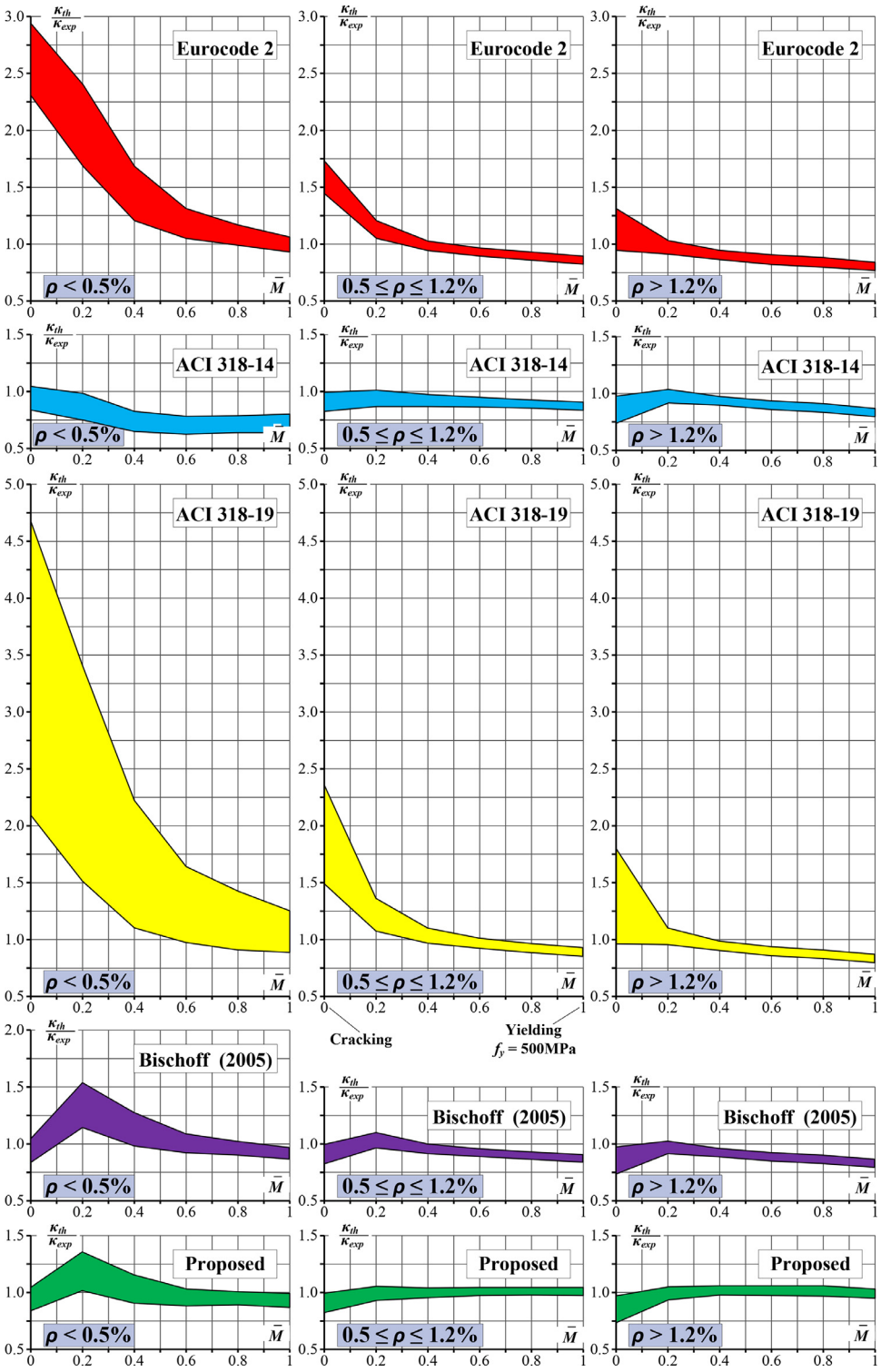

Fig. 6. 95% confidence intervals of the normalized curvature.

69 RC beams having a rectangular section and subjected to four-point bending. The comparison to test data was performed for several intervals of reinforcement ratio and load intensity and included four other models (ACI 318-14, 2014; ACI 318-19, 2019; CEN, 2004; Bischoff, 2005). The obtained results are summarised below:

5) The prediction accuracy in terms of the mean values and the coefficient of variation differed for the considered curvature models as well as for ranging reinforcement ratios and load intensities. Greater scatter was obtained by all the methods for the members having low reinforcement ratios ($\rho < 0.5\%$), particularly at the early cracking stages.
6) The previous and current versions of the ACI design code differently predicted the curvature of lightly reinforced members. While ACI 318-14 has shown too stiff response throughout most of the loading stages, ACI 318-19 considerably overestimated the curvatures, particularly at the early stage of cracking. For various intervals of reinforcement ratio and load intensity, ACI 318-19 demonstrated similar curvature prediction tendencies to those of Eurocode 2.

7) At higher loads, design codes and Bischoff's model underestimated the curvature of the beams having moderate ($0.5 \le \rho \le 1.2\%$) and high ($\rho > 1.2\%$) reinforcement ratios. As the current study included only a limited number of the specimens with a high reinforcement ratio, future studies should aim to investigate heavily reinforced members.
8) The proposed model demonstrated consistent prediction results, with the mean normalized curvature (κ_{th}/κ_{exp}) being close to unity, independent of the reinforcement ratio and load level (except for cracking point, $\bar{M} = 0$). In most cases, the proposed model showed superiority over design code techniques in terms of the coefficient of variation. Future studies should be dedicated to improving the predictions of crack resistance.
9) The predictions of Bischoff's technique for lightly reinforced members were similar to those by the proposed model, whereas for the beams having moderate and large reinforcement ratio, they were almost identical with the results obtained by ACI 318-14.

Declaration of Competing Interest

The authors declare that there is no conflict of interest in association with the reported works in this paper.

Acknowledgement

This project has received funding from European Social Fund (Project No. 09.3.3-LMT-K-712-01-0145) under a grant agreement with the Research Council of Lithuania (LMTLT).

References

ACI 318-14, 2014. Building Code Requirements for Structural Concrete (ACI 318-14) and Commentary (ACI 318R-14). ACI Committee 318. Farmington Hills, MI, USA, p. 520.
ACI 318-19, 2019. *Building Code Requirements for Structural Concrete (ACI 318-19) and Commentary*. ACI Committee 318. Farmington Hills, MI, USA, p. 628.
Artemjev, V.P., 1959. Investigation of Strength, Stiffness and Crack Resistance of Reinforced and Prestressed Concrete Beams Ph.D thesis. V.V. Kuibyshev Moscow Institute of Civil Engineering, Moscow.
Belarbi, A., Hsu, T.T.C, 1994. Constitutive laws of concrete in tension and reinforcing bars stiffened by concrete. ACI Struct. J. 91 (4), 465–474. doi:10.14359/4154.
Bischoff, P.H., 2005. Reevaluation of deflection prediction for concrete beams reinforced with steel and fiber reinforced polymer bars. *J. Struct. Eng., ASCE* 131 (5), 752–767. doi:10.1061/(ASCE)0733-9445(2005)131:5(752).
Bischoff, P.H., Scanlon, A., 2007. Effective moment of inertia for calculating deflections of concrete members containing steel reinforcement and fiber-reinforced polymer reinforcement. ACI Struct. J. 104 (8), 68–75.
Branson, D. E. (1965). *Instantaneous and time-dependent deflections of simple and continuous reinforced concrete beams*. HPR Report No. 7, Part 1, Alabama Highway Department, Bureau of Public Roads, Alab. (Dept. of Civil Engineering and Auburn Research Foundation, Auburn Univ., Aug. 1963), 78 p.
CEN, 2004. Eurocode 2: Design of Concrete Structures – Part 1-1: General Rules and Rules for Buildings (EN 1992-1-1:2004). European Committee for Standardization: Brussels, Belgium.
Clark, L.A., Speirs, D.M., 1978. Tension Stiffening in Reinforced Concrete Beams and Slabs Under Short-Term Load. Cement and Concrete Association, London TR 42.521.
CEB, 2013. CEB-FIP Model Code 2010: Model Code for Concrete Structures. Ernst & Sohn, Wiley, Berlin, Germany, p. 434.
Considére, A., 1899. Influence of metal reinforcement on the properties of mortar and concrete. Le Genie Civil 22 (1), 229–233 (in French).
Figarovskij, V.V., 1962. Experimental Investigation of Stiffness and Cracking of Reinforced Concrete Flexural Members Subjected to Short-Term and Long-Term Loading Ph.D. thesis. NIIZhB, Moscow.
Ghali, A., Favre, R., Elbadry, M., 1986. Concrete Structures: Stresses and Deformations: Analysis and Design for Serviceability. Chapman & Hall, London.
Gilbert, R.I., 1999. Deflection calculations for reinforced concrete structures – why we sometimes get it wrong. Int. Concrete Abstr. Portal 96 (6), 1027–1032.
Gilbert, R.I., 2001. Deflection Calculation and Control – Australian Code Amendments and Improvements. American Concrete Institute, Farmington Hills, Mich, pp. 45–77 Code provisions for deflection control in concrete structures, SP-203E. G. Nawy and A. Scanlon, Eds..
Gilbert, R.I., 2006. Discussion of "Reevaluation of deflection prediction for concrete beams reinforced with steel and fiber reinforced polymer bars" by Peter H. Bischoff. J. Struct. Eng., ASCE 132 (8), 1328–1330. doi:10.1061/(ASCE)0733-9445(2006)132:8(1328).
Gilbert, R.I., Warner, R.F., 1978. Tension stiffening in reinforced concrete slabs. J. Struct. Div. 104 (12), 1885–1900. doi:10.1061/(ASCE)0733-9445(2007)133:6(899).
Gribniak, V., 2009. Shrinkage Influence on Tension–Stiffening of Concrete Structures Ph.D. Thesis. Vilnius Gediminas Technical University, Vilnius, Lithuania.
Gribniak, V., Cervenka, V., Kaklauskas, G., 2013. Deflection prediction of reinforced concrete beams by design codes and computer simulation. Eng. Struct. 56, 2175–2186. doi:10.1016/j.engstruct.2013.08.045.
Kaklauskas, G., Christiansen, M.B., Bacinskas, D., Gribniak, V., 2008. Deformation Model of Reinforced Concrete Members Taking Into Consideration Shrinkage and Creep Effects at the Pre-Loading Stage. Vilnius Gediminas Technical University, Vilnius Final Report No T-1025/08[in Lithuanian].
Kaklauskas, G, Ghaboussi, J, 2001. Stress-strain relations for cracked tensile concrete from RC beam tests. J. Struct. Eng., ASCE 127 (1), 64–73. doi:10.1061/(ASCE)0733-9445(2001)127:1(64).
Kaklauskas, G., Gribniak, V., 2011. Eliminating shrinkage effect from moment-curvature and tension-stiffening relationships of reinforced concrete members. J. Struct. Eng., ASCE 137 (12), 1460–1469. doi:10.1061/(ASCE)ST.1943-541X.0000395.
Kaklauskas, G., Gribniak, V., 2016. Hybrid tension stiffening approach for decoupling shrinkage effect in cracked reinforced concrete members. J. Eng. Mech., ASCE 142 (11). doi:10.1061/(ASCE)EM.1943-7889.0001148, 04016085.
Kaklauskas, G., Gribniak, V., Bacinskas, D., Sokolov, A, et al., 2011a. Modelling of the Interaction Between Reinforcement and Concrete: A Unified Concept. Vilnius Gediminas Technical University, Vilnius Final Report No MIP-126/2010[in Lithuanian].
Kaklauskas, G., Gribniak., V, Salys, D., Sokolov, A., Meskenas, A, 2011b. Tension stiffening model attributed to tensile reinforcement for concrete flexural members. Proc. Eng. 14, 1433–1438. doi:10.1016/j.proeng.2011.07.180.
Kaklauskas, G., Sokolov, A., Bacinskas, D., Rumsys, D., Jakubovskis, R., Bado, M.F., 2019. Enhancing Durability of Concrete Structures: Innovative Concept of Crack Analysis. Vilnius Gediminas Technical University, Vilnius Interim Report No 09.3.3-LMT-K-712-01-0145[in Lithuanian].
Mörsch, E., 1909. Concrete-Steel Construction. Engineering News Publishing Company, New York Mc-Graw Hill, 368 p.
Murashev, V.I., 1950. Crack Resistance, Stiffness and Strength of Reinforced Concrete. Mashinostroyizdat, p. 286 (in Russian).
Salys, D., 2011. Modelling of Tensile Zone Behaviour of Reinforced Concrete Members Ph.D. Thesis. Vilnius Gediminas Technical University, Vilnius, Lithuania.
Scanlon, A., Bischoff, P.H., 2008. Shrinkage restraint and loading history effects on deflection of flexural members. ACI Struct. J. 105 (4), 498–506.
Scanlon, A., Cagley Orsak, D.R., Buettner, D.R., 2001. *ACI Code Requirements for Deflection Control: A Critical Review*. SP203-01. American Concrete Institute, Farmington Hills, Michigan, pp. 1–13.
Torres, L., Barris, C., Kaklauskas, G., Gribniak, V., 2015. Modelling of tension-stiffening in bending RC elements based on equivalent stiffness of the rebar. Struct. Eng. Mech. 53 (5), 997–1016 http://dx.doi.org/10.12989/sem.2015.53.5.997.